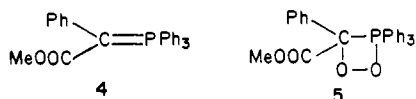


decomposition to form dioxetane **3c** as second intermediate by loss of nitrogen.<sup>9</sup> At  $-80\text{ }^\circ\text{C}$ , however, the pseudorotation in **3c** occurs within the time scale of the NMR experiment. This phosphadioxetane might be responsible for the chemiluminescence similar to the case of dioxetanes.<sup>19</sup>

Parallel  $^{31}\text{P}$  NMR studies were carried out for the direct observation of phosphadioxetane which could be derived from photooxygenation of phosphonium ylides.<sup>20</sup> The reaction mixture of photooxygenation of  $[\alpha\text{-(methoxycarbonyl)benzylidene}]$ triphenylphosphorane<sup>21</sup> (**4**,  $2.4 \times 10^{-1}\text{ M}$ ) gave a  $^{31}\text{P}$  NMR spectrum ( $-107\text{ }^\circ\text{C}$ ) featuring pairs of singlets at  $-25.8$  and  $-26.9$  ppm in a ratio of 0.9:1, respectively, together with two other singlets: 25.8 (triphenylphosphine oxide) and 20.8 ppm (unreacted **4**). On



warming to  $27\text{ }^\circ\text{C}$ , both upfield peaks disappeared. We can assign such upfield peaks as those of the conformers of dioxetane **5**<sup>16,23,24</sup> similar to the case of diazine **2c**.

**Acknowledgment.** We thank Y. Nagai, Eisai Company Co., Ltd., for measurement of the high-field  $^{31}\text{P}$  NMR spectra.

(19) See, for example: (a) Gunderman, K. D. "Chemiluminescence and Bioluminescence"; Plenum Press: New York, 1973. (b) Schaap, A. P.; Zaklika, K. A. "Singlet Oxygen"; Wasserman, H. H., Murray, R. W., Ed.; Academic Press: New York, 1979; p 174. (c) Schuster, G. B. *Acc. Chem. Res.* **1979**, *12*, 366.

(20) Jefford, C. W.; Barchietto, G. *Tetrahedron Lett.* **1977**, 4531.

(21) Bestman, H. J.; Schultz, H. *Justus Liebigs Ann. Chem.* **1964**, 674, 11.

(22) When the reaction mixture was warmed to room temperature with 9,10-diphenylanthracene, a very weak light emission was observed.

(23) De'Ath, N. J.; Denny, D. Z.; Denny, D. B. *J. Chem. Soc., Chem. Commun.* **1972**, 272.

(24) An approximate value of  $k_c$  is  $4 \times 10^2\text{ s}^{-1}$ .<sup>16b</sup>

## Phase Transitions Affecting Intramolecular Electron Transfer in Mixed-Valence Trinuclear Iron Acetate Complexes<sup>1</sup>

Seung M. Oh, Takeshi Kambara,<sup>2</sup> and David N. Hendrickson\*

School of Chemical Sciences, University of Illinois  
Urbana, Illinois 61801

Michio Sorai\* and Kazutoshi Kaji

Chemical Thermodynamics Laboratory  
Faculty of Science, Osaka University  
Toyonaka, Osaka 560, Japan

Scott E. Woehler and Richard J. Wittebort\*

Department of Chemistry, University of Louisville  
Louisville, Kentucky 40292  
Received May 17, 1985

In a recent paper<sup>3</sup> we suggested that in the solid state the ability of one of the three 4-ethylpyridine ligands of oxo-centered  $[\text{Fe}_3\text{O}(\text{O}_2\text{CCH}_3)_6(4\text{-Et-py})_3](4\text{-Et-py})$  to move between two positions as the temperature of the crystal was increased controlled

(1) A part of this paper corresponds to Contribution No. 89 from the Chemical Thermodynamics Laboratory.

(2) On sabbatical leave from the Department of Engineering Physics, The University of Electro-Communications, Tokyo, Japan.

(3) Oh, S. M.; Hendrickson, D. N.; Hassett, K. L.; Davis, R. E. *J. Am. Chem. Soc.* **1984**, *106*, 7984-7985.

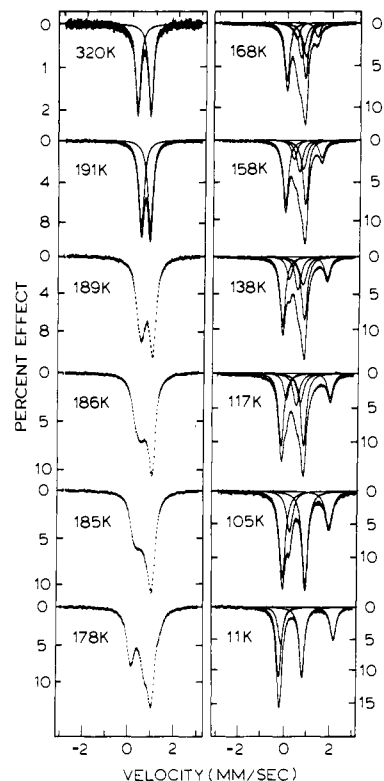


**Figure 1.** Variable-temperature  $^{57}\text{Fe}$  Mössbauer spectra for  $[\text{Fe}_3\text{O}(\text{O}_2\text{CCH}_3)_6(\text{py})_3](\text{py})$ . Velocity scale is referenced to iron foil at room temperature.

the rate of intramolecular electron transfer in the mixed-valence  $\text{Fe}_3\text{O}$  complex. In this paper direct evidence will be presented for the presence of phase transitions in  $[\text{Fe}_3\text{O}(\text{O}_2\text{CCH}_3)_6(\text{py})_3](\text{py})$  (**1**) that affect the rate of intramolecular electron transfer.

Compound **1** is isostructural with the analogous manganese compound.<sup>4,5</sup> In the room-temperature space group  $R\bar{3}2$  the  $\text{Fe}_3\text{O}$  triangular complexes are arranged in stacks with  $C_3$  axes oriented down the stacks. Ongoing single-crystal X-ray work<sup>6</sup> shows that the pyridine solvate molecules are sandwiched between the  $\text{Fe}_3\text{O}$  complexes in the stacks. The plane of the solvate molecule is perpendicular to the  $\text{Fe}_3\text{O}$  plane. At room temperature the pyridine solvate molecules are disordered in three positions about the  $C_3$  axis.

Variable-temperature Mössbauer spectra for **1** are shown in Figure 1. At temperatures below  $\sim 100\text{ K}$ , two quadrupole-split doublets are seen, one characteristic of high-spin  $\text{Fe}^{\text{II}}$  and the other of high-spin  $\text{Fe}^{\text{III}}$ . As the sample temperature is increased from 11 K, the first appreciable change in the spectrum is seen at  $\sim 117\text{ K}$ , where a third doublet appears. The spectrum changes dramatically as the temperature is further increased, eventually to become a single average doublet<sup>7</sup> at temperatures above  $\sim 190\text{ K}$ . It is clear that the rate of intramolecular electron transfer is increasing with increasing temperature. Above  $\sim 190\text{ K}$  it exceeds the  $\sim 10^7\text{--}10^8\text{ s}^{-1}$  rate which the Mössbauer technique can sense.

The heat capacity at constant pressure was measured for a 17.7794-g sample of **1** from 12 to 300 K. As can be seen in Figure 2, there are basically two phase transitions present, a first-order

(4) Baikie, A. R. E.; Hursthouse, M. B.; New, D. B.; Thornton, P. *J. Chem. Soc., Chem. Commun.* **1978**, 62.

(5) See Table III in: Catterick, J.; Thornton, P. *Adv. Chem. Radiochem.* **1977**, *20*, 291.

(6) Strouse, C. E.; Hendrickson, D. N.; Oh, S. M., unpublished results.

(7) Evidence for the fact that the single doublet seen in the 320 K spectrum is the average of the two doublets seen in the 11 K spectrum can be taken from the isomer shift data. At 320 K the single doublet has  $\delta$  0.753 (1) mm/s. At 11 K the  $\text{Fe}^{\text{II}}$  doublet has  $\delta$  1.260 (2) mm/s and the  $\text{Fe}^{\text{III}}$  doublet has  $\delta$  0.521 (1) mm/s; the average of these two doublets gives  $\delta$  0.767 mm/s.

(8) Kambara, T.; Sorai, M.; Oh, S. M.; Hendrickson, D. N., unpublished results.

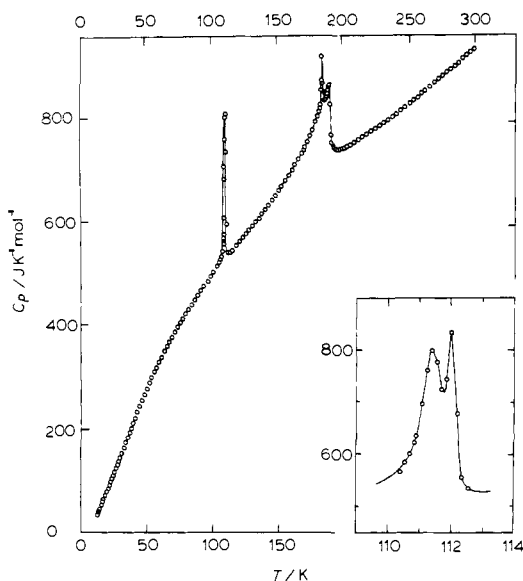


**Figure 2.** Plot of heat capacity at constant pressure,  $C_p$ , as a function of temperature. The inset shows an expanded view of the low-temperature heat capacity effect.

phase transition with two  $C_p$  peaks at 111.4 and 112.0 K and a higher order phase transition with two  $C_p$  peaks at 185.8 and 191.3 K. It is very interesting that the temperature of the 111–112 K phase transition occurs at the temperature where the first Mössbauer spectrum change occurs. The higher order phase transition can be seen to evolve over a large temperature range with  $C_p$  peaks at the temperature where the Mössbauer spectrum becomes a single average doublet.

It is suggested that the lower temperature phase transition is an order–disorder phase transition. At temperatures below this first phase transition the triangular complexes each have a static distortion reflecting the iron valence states. One iron is  $\text{Fe}^{\text{II}}$  and the other two are  $\text{Fe}^{\text{III}}$ . These distorted complexes are ordered in domains, e.g., homogeneous regions of crystallite where the distortions of the  $\text{Fe}_3\text{O}$  units are ordered in the same sense. At the low-temperature phase transition these domains disappear and the sense of distortion becomes randomly distributed throughout the crystallite. Cooperativity is the essence of a phase transition. The packing arrangement in **1** involves stacks of pyridine ligands with an interplanar separation of  $c/3 = 3.5 \text{ \AA}$ . The pyridine ligands from neighboring molecules experience appreciable  $\pi$ – $\pi$  overlap and this could lead to cooperativity and the first-order phase transition at 111–112 K. In a later paper<sup>8</sup> it will be shown that the third doublet that appears in the Mössbauer spectrum (see Figure 1) at  $\sim 117 \text{ K}$  is attributable to  $\text{Fe}_3\text{O}$  complexes that are electronically delocalized. The first-order phase transition at  $\sim 112 \text{ K}$  leads to a change in the potential energy diagram such that above this temperature the zero point energies of the delocalized and localized complexes become comparable in magnitude.

The higher temperature phase transition is not first order, for it evolves over an extensive temperature range. It is likely that this phase transition involves  $\text{Fe}_3\text{O}$  molecules becoming thermally activated to change their sense of distortion combined eventually with the pyridine solvate molecules starting to rotate about the  $C_3$  axes of the stacks of  $\text{Fe}_3\text{O}$  molecules. Preliminary single-crystal X-ray diffraction work<sup>6</sup> indicates that the  $C_3$  axis disappears at  $\sim 190 \text{ K}$  as the crystal is cooled from 300 K.

Definitive evidence for the motion of solvate molecules in the solid state has been determined for compound **2**,  $[\text{Fe}_3\text{O}(\text{O}_2\text{CCH}_3)_6(4\text{-CH}_3\text{-py})_3](\text{C}_6\text{D}_6)$ , where the solvate molecule is a deuterated benzene. Compound **2** is isostructural with **1** and shows a similar temperature dependence in its Mössbauer spectrum. A complete single-crystal  $^2\text{H}$  NMR study has been carried out on **2** at room temperature. Rotations were carried out about three orthogonal axes. At every setting of the single crystal only a single quadrupole-split doublet is seen. It is clear that the  $\text{C}_6\text{D}_6$

molecule is rapidly rotating about a 6-fold axis to make all deuterium sites equivalent. The principal components of the deuterium quadrupole interaction tensor were found to be  $-13.5 \pm 0.5$ ,  $-18.3 \pm 0.5$ , and  $+31.6 \pm 0.5 \text{ kHz}$ . These values are considerably reduced from what is expected for a  $\text{C}_6\text{D}_6$  fixed in the solid in which case the axially symmetric principal components are  $-67$  and  $135 \text{ kHz}$ . Reorientation about the  $C_3$  axis along the molecular stacks or about a  $C_2$  axis perpendicular to it is also present in addition to the rotation about the 6-fold axis.

Variable-temperature IR studies of **1**, isostructural  $[\text{Fe}_2^{\text{III}}\text{Co}^{\text{II}}\text{O}(\text{O}_2\text{CCH}_3)_6(\text{py})_3](\text{py})$ , and symmetric  $[\text{Fe}^{\text{III}}_3\text{O}(\text{O}_2\text{CCH}_3)_6(\text{py})_3]\text{ClO}_4$  clearly indicate, based on the  $\text{M}_3\text{O}$  asymmetric stretch regions, that compound **1** is “valence localized” in terms of the IR experiment in the 500–800- $\text{cm}^{-1}$  region. Thus, **1** and the  $\text{Fe}^{\text{III}}_2\text{Co}^{\text{II}}$  complex each show two asymmetric stretches, whereas, the higher symmetry  $\text{Fe}^{\text{III}}_3$  complex exhibits one such band. This same conclusion was reached by Cannon et al.<sup>9</sup> At or above the higher temperature phase transition, the pyridine solvate molecules are rotating and the  $\text{Fe}_3\text{O}$  molecules are changing their sense of distortion much faster than can be sensed by the Mössbauer technique but slower than would average the two  $\text{Fe}_3\text{O}$  asymmetric stretching bands.

Dynamics in the solid state involving the onset of motion in a ligand, solvate molecule, or counterion at a certain temperature could in general be major factors determining whether the intramolecular electron transfer in a given mixed-valence complex is fast or slow. We have also detected phase transitions for the mixed-valence complex  $[\text{Fe}_3\text{O}(\text{O}_2\text{CCH}_3)_6(3\text{-CH}_3\text{-py})_3](3\text{-CH}_3\text{-py})$ ,<sup>10</sup> which has a different solid-state structure than **1**, and for mixed-valence biferricenium triiodide.<sup>11</sup>

**Acknowledgment.** We thank the National Institutes of Health for support of the work at the University of Illinois through Grant HL13652 to D.N.H. and the National Science Foundation (P. C.M. 8118912 to R.J.W.) for the work at the University of Louisville.

(9) Cannon, R. D.; Montri, L.; Brown, D. B.; Marshall, K. M.; Elliott, C. M. *J. Am. Chem. Soc.* **1984**, *106*, 2591.

(10) Sorai, M.; Shiomi, Y.; Hendrickson, D. N.; Oh, S. M., unpublished results.

(11) Sorai, M.; Hendrickson, D. N.; Dong, T.-Y.; Cohn, M. J., unpublished results.

## Stereoselective Synthesis of $\gamma,\delta$ -Epoxy- $\beta$ -methyl- $\gamma$ -(trimethylsilyl)alkanols. Synthesis of the C(1)–C(7) Segment of 6-Deoxyerythronolide B

Yuichi Kobayashi, Hiroshi Uchiyama, Hiroshi Kanbara, and Fumie Sato\*

Department of Chemical Engineering  
Tokyo Institute of Technology  
Meguro, Tokyo 152, Japan

Received April 8, 1985

Previously, we have reported a highly enantio- and diastereoselective synthesis of *syn*- and *anti*- $\beta$ -methyl- $\gamma$ -(trimethylsilyl) homoallyl alcohols **1** and **2**.<sup>1</sup> In connection with ongoing program directed toward the utilization of these alcohols for synthesis of naturally occurring acyclic molecules such as macrolide and ionophore antibiotics, we have been interested in stereoselective synthesis of four possible diastereoisomers of  $\gamma,\delta$ -epoxy- $\beta$ -

(1) (a) Sato, F.; Kusakabe, M.; Kobayashi, Y. *J. Chem. Soc., Chem. Commun.* **1984**, 1130. (b) Kobayashi, Y.; Kitano, Y.; Sato, F. *Ibid.* **1984**, 1329. (c) Sato, F.; Kusakabe, M.; Kato, T.; Kobayashi, Y. *Ibid.* **1984**, 1331.